Tropical Biomedicine 42(3): 258-266 (2025)
https://doi.org/10.47665/tb.42.3.004

RESEARCH ARTICLE

The efficiency of non-thermal plasma on the inhibition of environmental isolates of *Cryptococcus neoformans* from pigeon droppings

Buppan, P.[1], Saengchan, N.[1], Thongma, K.[1], Phuangphuang, P.[1], Sangwang, W.[2], Matra, K.[3*]

[1]Department of Health Promotion, Faculty of Physical Therapy, Srinakharinwirot University, Nakhonnayok, Thailand
[2]Thailand Institute of Nuclear Technology (Public Organization), Nakhonnayok, Thailand
[3]Department of Electrical Engineering, Faculty of Engineering, Srinakharinwirot University, Nakhonnayok, Thailand
*Corresponding author: Khanit@g.swu.ac.th

ARTICLE HISTORY

Received: 12 April 2025
Revised: 7 May 2025
Accepted: 29 May 2025
Published: 30 September 2025

ABSTRACT

This study evaluated the antifungal efficacy of a non-thermal plasma (NTP) jet against environmental isolates of *Cryptococcus neoformans*, a pathogenic fungus commonly found in pigeon droppings and associated with serious infections in immunocompromised individuals. Given the increasing concern over environmental fungal contamination and drug-resistant strains, this research aimed to identify optimized plasma conditions for effective fungal inactivation without relying on chemical disinfectants. Environmental *C. neoformans* isolates were cultured on Sabouraud dextrose agar and subjected to NTP treatment under systematically varied parameters: input power (30, 50, and 70 W), exposure time (30 s, 1, 2, and 3 min), and air flow rates (1, 1.5, and 2 LPM) mixed with a constant 12 LPM argon gas. Following treatment, plates were incubated at 37°C for 24 hours, and antifungal activity was assessed by measuring the inhibition zone. The highest antifungal effect was achieved at 70 W, with a 3-minute exposure and Ar:Air flow ratio of 12:2 LPM, producing a clear zone of 0.93 ± 0.05 cm^2. This value corresponded to 28.6% of the inhibition zone produced by the Amphotericin B positive control (3.25 ± 0.08 cm^2). All treatment conditions exhibited statistically significant inhibition ($p < 0.05$), with increased efficacy at higher airflow and longer exposure durations. The generation of reactive oxygen and nitrogen species (RONS) is believed to be the primary mechanism underlying fungal inactivation. These findings demonstrate that Argon-Air-based NTP jet systems offer a promising, eco-friendly, and non-chemical approach for controlling fungal pathogens in environmental settings. The method has potential for application in urban sanitation and public health contexts where fungal contamination from bird droppings poses ongoing risks.

Keywords: *Cryptococcus neoformans*; non-thermal plasma; reactive oxygen and nitrogen species (RONS); environmental disinfection; pigeon droppings.

INTRODUCTION

Cryptococcus neoformans (*C. neoformans*), characterized by its encapsulated opportunistic yeast morphology with diameters typically ranging from 2.5 to 8.0 microns, boasts a ubiquitous global distribution (Zhao *et al*., 2023). Its predominance, notably concentrated among pigeon populations, extends beyond avian habitats to encompass various environments, including bird droppings, chicken coops, arboreal settings, soil, and the ambient atmosphere (Buppan *et al*., 2017; Watkins *et al*., 2017; Madsen *et al*., 2022). This prevalence is especially pronounced in regions such as Thailand. Humans can contract the infection directly through contact with pigeons or indirectly through interactions with pigeon-derived secretions, such as feces, mucus, tears, and saliva. This complex interaction underscores the intricate transmission dynamics of *C. neoformans* concerning human health. Pigeon droppings, a major reservoir of *C. neoformans*, frequently accumulate in diverse urban and suburban environments, including public parks, historic buildings, rooftops, balconies, and residential areas. These locations often serve as habitats where pigeons nest and feed, increasing the likelihood of fungal contamination and subsequent exposure to humans. The presence of this pathogen in community settings highlights a significant environmental health issue. The pathogen is of notable public health importance, capable of causing severe diseases in humans, such as pulmonary cryptococcosis leading to fungal pneumonia, and central nervous system cryptococcosis resulting in fungal brain infections and meningitis. Additionally, infections can manifest on the skin, often resembling acne, a condition known as cutaneous and mucocutaneous cryptococcosis (Buppan *et al*., 2017; Watkins *et al*., 2017; Madsen *et al*., 2022; Zhao *et al*., 2023; Pal *et al*., 2024).

Currently, there exists no direct therapeutic intervention for diseases stemming from *C. neoformans*; only symptomatic management is accessible. Efforts to manage infections have primarily

concentrated on three classes of antifungal drugs: polyenes, azoles, and a pyrimidine-derived medication. Unfortunately, some of these treatment options exhibit high failure rates, and the emergence of intrinsic fungal resistance is a growing concern (Morrison, 2006; Zaragoza *et al*., 2009; Krangvichain *et al*., 2016; Iyer *et al*., 2021). Moreover, existing antifungal treatments often entail significant side effects and environmental risks associated with chemical residues. Therefore, innovative alternative methods with fewer side effects and environmental impacts are critically needed.

Recently, low-temperature plasma, also known as non-thermal plasma, has garnered significant attention within the research community. The unique characteristics of plasma, including free space charges and free radicals (especially reactive oxygen and nitrogen species, RONS), make it a versatile tool with applications spanning various fields, such as biomedicine, materials science, nanoparticle synthesis, agriculture, and microbial disinfection (Seelarat *et al*., 2024; Xu *et al*., 2024; Chanchula *et al*., 2025; Matra *et al*., 2025; Panklai *et al*., 2025; Thana *et al*., 2025a). Notably, low-temperature plasma presents an intriguing avenue for inhibiting the growth of fungi, bacteria, and viruses. Prior studies have successfully demonstrated the efficacy of non-thermal plasma in microbial inactivation, including bacteria and certain fungi. revealed that plasma-activated water and atmospheric-pressure plasma could inactivate viruses by disrupting viral structures through RONS generation, indicating its broad-spectrum antimicrobial capacity (Guo *et al*., 2018). In terms of fungal control, Sun et al. demonstrated that non-thermal plasma significantly reduced Candida biofilms and even enhanced the fungistatic effect of conventional antifungal drugs (Sun *et al*., 2012). Similarly, showed that non-thermal dielectric-barrier discharge plasma could effectively eliminate methicillin-resistant Staphylococcus aureus (MRSA), both in planktonic and biofilm states, suggesting its potential for controlling biofilm-associated pathogens (Joshi *et al*., 2010). Furthermore, reviewed the applicability of non-thermal plasma in wound healing and noted its promising antifungal and antibacterial properties, which support its utility in clinical and environmental disinfection contexts (Haertel *et al*., 2014).

However, the specific application of non-thermal plasma against environmental isolates of pathogenic fungi, particularly *C. neoformans* derived directly from pigeon droppings a significant source of human infection remains inadequately explored. Most previous studies related to fungal inactivation by plasma were conducted under controlled laboratory conditions using standard reference strains rather than environmental isolates. This represents a significant research gap, as environmental isolates often exhibit different resistance profiles and characteristics compared to laboratory strains (Handorf *et al*., 2018; Ito *et al*., 2020; Nimbua *et al*., 2020; Chen *et al*., 2022; Andriani *et al*., 2023; Zhao *et al*., 2023).

To address this crucial research gap, our study uniquely focuses on investigating the inhibitory efficacy of a non-thermal plasma jet specifically against environmental isolates of *C. neoformans* collected from pigeon droppings. Moreover, unlike previous research that primarily relied on single gas plasma systems, this research systematically evaluates the synergistic effect of Argon-Air mixed gases on the inactivation efficiency, exploring multiple operational parameters, including input power, exposure duration, and gas flow rates. This comprehensive evaluation aims to optimize the application conditions of non-thermal plasma for effective environmental pathogen control.

MATERIALS AND METHODS

Plasma jet model and experimental setup

Figure 1 illustrates the schematic representation of the plasma treatment setup. The plasma jet model features a tungsten anode electrode with a 1Ø mm tip, centrally inserted into a 3-ways quartz tube from the top. The plasma jet device comprises a quartz tube measuring 180 mm in length, with inner and outer diameters of 4 mm and 6 mm, respectively. A tungsten anode, with a total length of 195 mm and a fine 0.1 mm-diameter tip, is centrally inserted into the tube. The tip extends 10 mm beyond the end of the quartz tube, allowing direct exposure to ambient gas for efficient plasma jet formation. At the lower end of the quartz tube, a Teflon housing–configured in a bobbin-like shape–encases the tube to provide structural support and dielectric isolation. This housing includes a 10 mm-wide central shaft between two 15 mm-thick discs, forming a stable mounting base. A 0.1 mm-thick aluminum sheet cathode is tightly wrapped around the central shaft, forming the outer electrode in the coaxial configuration. Argon (Ar) and air mixed gas, carrier gas for plasma jet generation, have been supplied from the gas cylinders controlled by a flow meter, and was fed into the side-port situated at the upper end of the quartz tube via a plastic tube. Plasma generation was achieved by applying power from a custom-built 300 W resonant-type alternating current (AC) power supply, designed to match the dynamic impedance of the plasma load. In order to monitor the electrical characteristics, both discharge current (I_d) and voltage (V_d) parameters were observed. For I_d, a general-purpose passive probe was connected across a 100-ohm monitor resistor positioned before the ground, while a high-voltage probe (Pintek HVP-28HF) was connected between the plasma model and ground to observe V_d. The I_d and V_d measurements from both probes were displayed on an oscilloscope (Siglent SDS2304). To study optical emission spectroscopy (OES) during plasma jet generation, a small charge-coupled device (CCD) spectrometer (Newport 71SI00087) has been employed. The optical fiber detector tip was positioned 2 cm beneath the plasma jet. The experiments were carried out in an open indoor environment within a temperature-controlled study room maintained at approximately 25.0 ± 1.2°C using an air conditioning system. Based on regional climatological data for Onkharak District, Nakhon Nayok, Thailand during the month of experimental conduction period, the ambient relative humidity was estimated to range between 70–80%.

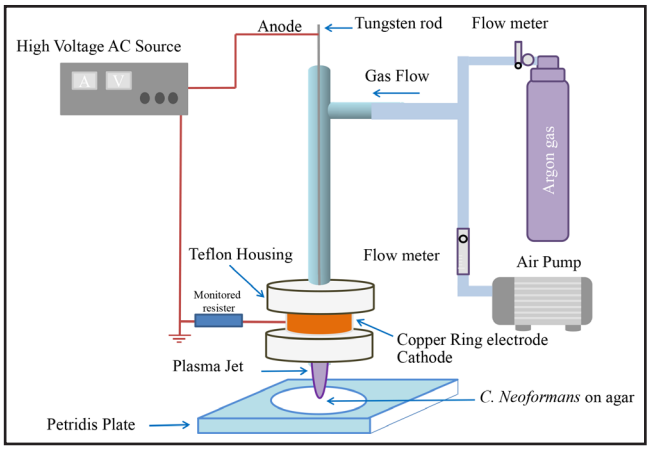

Figure 1. Experimental set up for treatment process.

In this paper, the studied parameters involved in microorganism inactivation have been varied, including the treatment input power (30 W, 50 W, 70 W), exposure duration (ranging from 30 s to 3 min), and airflow rates (ranging from 1, 1.5 and 2 LPM) mixed with 12 LPM of Ar gas.

Collection of pigeon droppings samples and detection of *Cryptococcus neoformans*

Cryptococcus neoformans was sampled from various sources, including pigeon droppings found in footpath areas, building balconies, and fire escape stairs at Srinakharinwirot University, Ongkharak Campus, Ongkharak District, Nakhon Nayok Province, Thailand. Scooping equipment was used to collect 5 g of each sample, which was then dissolved in 100 mL of 0.85% NaCl. After thorough shaking for 5 min, the mixture was left to settle for approximately 15 min. A volume of 100 µl of the clear supernatant was aspirated and cultured using the Spread plate technique on Sabouraud dextrose agar (SDA) medium supplemented with 0.4 g/L Chloramphenicol. The cultured plates were incubated at 37°C for 24 hours. Following incubation, opaque, smooth-edged, creamy-white mucous colonies were identified and streaked onto Cryptococcus differential agar. If the colonies were *C. neoformans*, they exhibited a distinct blue appearance.

Identification of *Cryptococcus neoformans* by biochemical testing method

The diagnosis of enzyme formation, specifically Phenoloxidase, involved isolating bacteria exhibiting suspicious colony characteristics and streaking them onto Caffeic acid agar. These cultures were then incubated at 37°C for 24 hours, where colonies of *C. neoformans* would typically display a brown coloration (Wang *et al*., 1977). For the diagnosis of Urease enzyme production, streaking was performed on Urea base agar followed by incubation at 37°C for 24 hours. In the case of *C. neoformans*, the culture medium would exhibit a pink coloration (Morrow & Fraser, 2013).

Preparing *Cryptococcus neoformans* for testing method

A single colony was extracted from the Sabouraud dextrose agar (SDA) medium and diluted with a 0.85% saline solution to create a bacterial suspension. The light absorption of the suspension was measured at a wavelength of 640 nm. The Optical Density (OD) was determined to be $1x10^8$ CFU/mL. Following this, 1 mL of the culture was extracted and spread across an SDA dish to further evaluate the efficacy of low-temperature plasma in eradicating *C. neoformans*.

Investigation of the fungicidal activity of low-temperature plasma on *Cryptococcus neoformans*

To assess the efficacy of low-temperature plasma against *C. neoformans*, various parameters were configured: argon gas flow rates of 12 LPM, combined with three air flow rates (1 LPM, 1.5 LPM, and 2 LPM); three power settings (30 W, 50 W, and 70 W); and four different time durations (30 s, 1 min, 2 min, and 3 min). The *C. neoformans* colonies cultured on Sabouraud dextrose agar (SDA) were exposed to these specific plasma jet conditions at a 20 mm distance from the plasma jet reactor tip. The selected nozzle-to-surface distance, defined as the gap from the lower end of the quartz tube to the agar surface, was optimized to achieve a balance between plasma reactivity and surface safety. At shorter distances, excessive localized heating and desiccation of the culture medium were observed. In contrast, greater distances resulted in diminished reactive species density at the target surface, thereby reducing antifungal efficacy (Palee *et al*., 2023; Thana *et al*., 2025b). Higher gas flow rates were excluded to reduce argon consumption and prevent colony displacement under the open-tip geometry. Air alone was unsuitable as a working gas due to its high breakdown voltage; thus, argon was used to stabilize the discharge and promote ionization via the Penning effect. This mechanism enables energy transfer from metastable Ar to O_2 and N_2, enhancing ionization and RONS generation under moderate input power (Nimbua *et al*., 2020; Morabit *et al*., 2021; He *et al*., 2024). Subsequently, the samples were incubated at 37°C for 24 hours to observe and measure the resulting clear zones. Positive control was performed using Amphotericin B at standard concentrations known to exhibit strong inhibitory efficacy against *C. neoformans*. The clear zone measured after incubation (37°C for 24 hours) covered the entire plate, clearly demonstrating complete fungal inhibition. The clear zone measurements in the positive control group were significantly larger compared to all experimental conditions, confirming its validity as a reference for assessing plasma efficacy. Conversely, the negative control samples (untreated group) were not exposed to plasma treatment, and as expected, exhibited no inhibitory clear zone (0.00±0.00 cm^2) under all tested conditions.

Calculation of clear zone area

After incubation, the clear zone area indicating inhibition of *C. neoformans* growth was measured. The clear zone diameter was measured in centimeters (cm) using a Vernier caliper, by recording two perpendicular diameters and calculating the average. The clear zone area was then determined using the standard formula for the area of a circle in Eq. (1) (Zhao *et al*., 2023):

$$\text{Clear zone area (cm)}^2 = 0.25\pi \times (\text{average diameter})^2 \quad (1)$$

Statistical analysis

For statistical analysis, each experimental condition was conducted in triplicate. Descriptive statistics were used to evaluate the prevalence of *C. neoformans* isolated from pigeon droppings collected at various locations within Srinakharinwirot University, Ongkharak Campus. Inferential statistics were applied to assess the antifungal efficacy of low-temperature plasma under different voltage, exposure time, and gas flow conditions. A one-way analysis of variance (ANOVA) was performed to identify statistically significant differences among treatment groups. When the ANOVA indicated significance ($p < 0.05$), Tukey's Honestly Significant Difference (HSD) test was employed as the post hoc multiple comparison method to determine pairwise differences between treatment means.

RESULTS

Plasma jet characteristics; Visual Observations, Electrical characteristics, and Optical Emission Spectroscopy

Visual Observations

After applying sufficient power from a high-voltage AC source, a stable plasma jet was successfully generated within the coaxial region between the stainless-steel anode tip and the aluminum cathode plate, and subsequently expelled along the gas flow axis. Figure 2 presents a comparative visual representation of plasma jet plume morphology under varying input powers (30, 50, and 70 W) and gas flow conditions. The top row shows jets produced using pure argon (12 LPM), while the subsequent rows depict the effects of incremental air admixture (1.0, 1.5, and 2.0 LPM) to the argon carrier gas.

At a constant argon flow rate, increasing input power results in a longer and brighter jet, indicating enhanced ionization and energy density. The addition of air significantly alters jet color and visible structure, suggesting a shift in plasma chemistry due to the presence of oxygen and nitrogen species. These changes are consistent with the transition from an inert argon discharge to a more reactive plasma environment. As seen in Figure 2, under the condition of 70 W input power, two representative plasma jet configurations were compared: a 12 LPM pure argon jet and a 12 LPM argon mixed with 2 LPM air jet, the pure argon plasma jet exhibits a bright bluish-violet plume enveloped by a diffuse purple glow, with an approximate length of 1.65 ± 0.21 cm measured from the nozzle tip. In contrast, the argon–air plasma jet appears as a more intense violet-blue emission, with a shorter axial extent of around 0.75 ± 0.13 cm. When the input power is reduced, the plasma jet correspondingly becomes dimmer and shorter. Furthermore, increasing air concentration results in progressively shorter jets with more pronounced violet coloration, consistent with higher levels of nitrogen and oxygen excitation and increased quenching effects (Nijdam *et al*., 2010; Niu *et al*., 2011; Nimbua *et al*., 2020; Su *et al*., 2021; Wei *et al*., 2023).

Electrical characteristics

To evaluate the electrical characteristics of the plasma jet system under varying gas compositions, discharge parameters were measured using a digital oscilloscope at input power levels of 30, 50, and 70 W. All measurements were conducted under atmospheric pressure within a coaxial electrode configuration comprising a stainless-steel anode and an aluminum cathode. Argon gas at a flow rate of 12 LPM was employed as the primary carrier gas, either in pure form or admixed with air at 1.0, 1.5, or 2.0 LPM. Representative discharge voltage and current waveforms were captured at input power levels of 30, 50, and 70 W using a digital oscilloscope. These waveforms exhibit quasi-sinusoidal behavior that becomes increasingly distorted with the addition of air, particularly at higher admixture levels. As shown in Figure 3, the waveforms at 70 W input power display increased distortion and irregular peak structures with rising air concentration–highlighting intensified streamer activity in reactive gas environments. These current spikes, superimposed on the base waveform, reflect the transition from a relatively diffuse discharge in pure argon to a more filamentary regime supported by the presence of electronegative species in the Ar–air mixture (Nijdam *et al*., 2010; Wei *et al*., 2023).

At 70 W input power, the average discharge power was calculated from the instantaneous voltage and current waveforms. For the pure argon condition, V_d,rms and I_d,rms were recorded at 4.86 ± 0.33 kV and 0.32 ± 0.03 mA, respectively, resulting in an average discharge power of 0.16 ± 0.01 W. With the addition of 1.0 LPM air, both voltage and current increased slightly to 5.21 ± 0.39 kV and 0.32 ± 0.02 mA, while the average power declined to 0.12 ± 0.01 W. In the Ar + Air 1.5 LPM condition, V_d,rms and I_d,rms further increased to 5.86 ± 0.41 kV and 0.35 ± 0.03 mA, yielding the highest discharge power of 0.20 ± 0.01 W. Under the Ar + Air 2.0 LPM condition, voltage and current remained comparable at 5.86 ± 0.45 kV and 0.34 ± 0.03 mA, respectively, resulting in a slightly elevated discharge power of 0.21 ± 0.02 W.

Analysis of waveform characteristics (Figure 3) highlights notable differences in discharge behaviour between gas compositions. In the case of pure argon, the discharge current displays low amplitude and irregular peak patterns, suggestive of a glow-like or diffuse discharge regime. By contrast, the introduction of air induces periodic, sharp current pulses synchronized with the applied voltage cycles–characteristic of streamer discharges. These results are consistent with increased plasma impedance due to oxygen-induced electron attachment and reduced electron mobility in nitrogen–oxygen mixtures. These results are consistent with increased plasma impedance due to oxygen-induced electron attachment and reduced electron mobility in nitrogen–oxygen mixtures. These results align

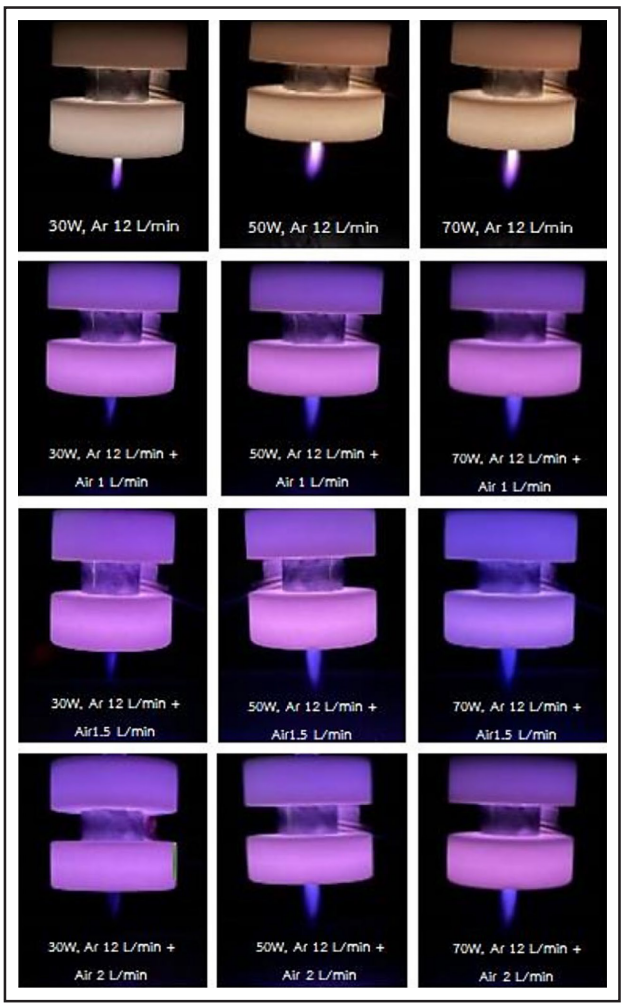

Figure 2. Visual plasma jet characteristics at various conditions.

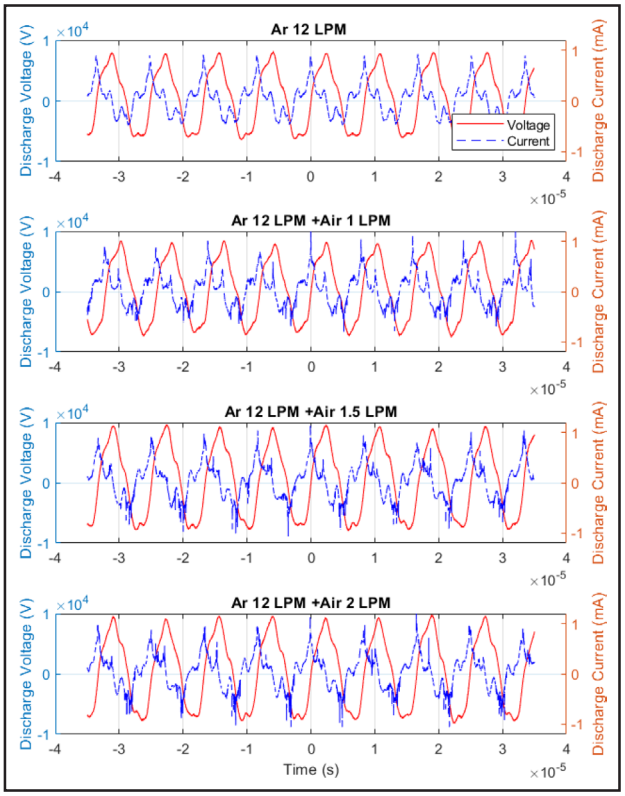

Figure 3. Comparison of the electrical characteristics of the plasma jet at an input power of 70 W under different gas compositions.

with the idea that adding oxygen increases plasma resistance by capturing free electrons and lowering their movement. The intensified and more regular current spikes observed at higher air concentrations indicate enhanced streamer activity, likely supported by electronegative species such as O_2 and N_2, which promote the formation of localized ionization channels (Nijdam *et al*., 2010; Nimbua *et al*., 2020; Su *et al*., 2021; Wei *et al*., 2023).

These observations confirm a shift in discharge regime from homogeneous plasma in pure argon to filamentary streamer discharges in Ar–air mixtures. Furthermore, the average discharge power consistently increased with higher input power across all gas. Although higher air content typically diminishes plasma conductivity due to increased electron attachment, the use of a resonance-type high-voltage power supply introduces a compensatory mechanism. Variations in the Ar–air ratio alter the complex impedance of the plasma load, thereby modulating the resonant condition of the power circuit. These impedance changes may enhance power coupling at specific gas compositions, mitigating the expected current reduction. Thus, the interplay between gas composition, discharge impedance, and resonant circuit dynamics plays a pivotal role in governing the electrical performance and discharge stability of the system (Ding *et al*., 2009; Su *et al*., 2021).

Optical Emission Spectroscopy

The OES analysis in Figure 4 revealed the presence of several reactive nitrogen species (RNS) and reactive oxygen species (ROS) that hold significance in microorganism inactivating contexts. While the overall OES trends in both cases appear quite similar, a notable discrepancy emerges when evaluating the intensity of the emissions. Specifically, it becomes evident that the pure Ar plasma jet demonstrates a notably stronger intensity in all detected OES measurements, particularly in the 690–850 nm region, where multiple Ar I transitions are observed, except for the N_2 second positive system (SPS, $C^3\Pi u \rightarrow B^3\Pi g$) in the 300–400 nm range. The prominent emission lines attributed to the hydroxyl (OH) radical band (306–315 nm) and atomic oxygen (776.7 nm) were identified (Ungwiwatkul *et al*., 2025). Furthermore, the OES data unveiled the distinct range featuring pronounced peaks (600–900 nm), which correspond to Ar-excited species, (Pan *et al*., 2015; Matra *et al*., 2023). These excited species play a significant role in the production of ROS, RNS, and RONS (reactive oxygen and nitrogen species). In the process of plasma jet generation, these species are produced, and they have the potential to serve as effective tools for microbial inactivation. The addition of air to the argon plasma jet notably enhanced the spectral features in the lower wavelength region, particularly the 290–390 nm range. These emissions are associated with the OH radical and the N_2 SPS, indicating the formation of chemically reactive plasma species. In contrast to pure Ar plasma, which is optically brighter due to intense Ar I lines, the Ar + Air plasma exhibited lower overall intensity but greater chemical richness due to enhanced generation of RONS (Qayyum *et al*., 2007; Garcia-Cosio *et al*., 2011; Nimbua *et al*., 2020). Notably, the species generated include ozone (O_3), OH radical, hydrogen peroxide (H_2O_2), nitric acid (HNO_3), nitrous acid (HNO_2), and peroxynitrous acid (ONOOH). These molecular species arise primarily from gas-phase reactions involving Ar collisions with N_2, O_2, and H_2O molecules present in the air admixture, especially within the high-energy discharge zone of the plasma jet (Ishaq *et al*., 2014; Yan *et al*., 2017; Cheng *et al*., 2020; Shi *et al*., 2023; Xu *et al*., 2024).

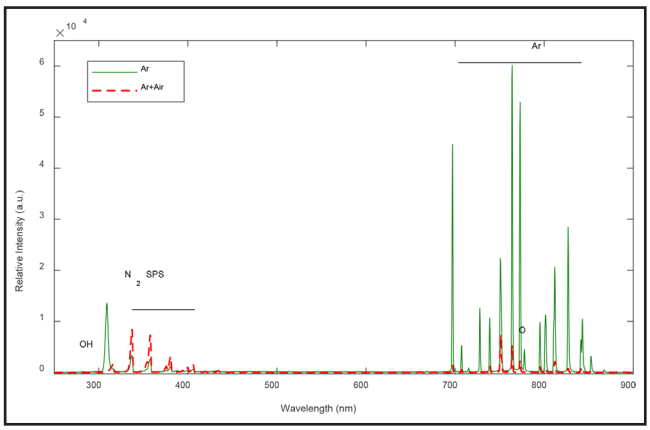

Figure 4. Comparative OES analysis of visual plasma jet characteristics: 12 LPM Ar and 12 LPM Ar with 2 LPM air, generated at 70 W_{input} in an open room environment.

Efficiency of non-thermal plasma on the inhibition of *C. neoformans*

Regarding the experimental findings on the average inactivation zone (clear zone) of *C. neoformans* presented in Table 1, it is evident that all tested plasma conditions contributed to fungal inactivation. A noticeable increase in the clear zone area was observed with longer exposure durations and higher air flow rates. Statistical analysis revealed significant differences in the clear zone areas across varying treatment times and air flow conditions, as indicated by the superscript values in Table 1. However, the effect of different input power levels was less pronounced, possibly due to inconsistencies in the in-house resonant power supply, which may have affected the output voltage and discharge characteristics non-linearly. The results highlight that the non-thermal plasma jet exhibited the highest antifungal efficacy when operated at 70 W input power, with an Ar:Air gas flow ratio of 12:2 LPM for 3 minutes. Under this condition, the maximum inhibition zone was recorded at 0.93 ± 0.05 cm², as illustrated in Figure 4. Compared to the positive control (Amphotericin B, clear zone = 3.25 ± 0.09 cm²), the optimal plasma condition achieved approximately 28.6% of the inhibition efficacy, indicating notable antifungal potential. In contrast, the negative control group exhibited no inhibition zone under any tested condition (0.00 ± 0.00 cm²). This substantial disinfection capacity is attributed to the ability of plasma-generated reactive species to catalyze oxidation reactions that compromise the structural integrity of the *C. neoformans* capsule.

However, upon detailed examination of Figure 5, it was observed that colony size significantly influenced the measurement of the clear zone area. Although all culture plates were incubated under identical conditions (37°C, 24 hours), colonies in the plates exposed to plasma for 3 minutes appeared noticeably larger compared to those exposed for only 30 seconds. This discrepancy in colony size directly impacts the apparent clear zone area, making it appear more pronounced in samples with initially larger colonies, despite the same initial colony number. Thus, the clear zone measurement might be subject to variability due to initial differences in colony size rather than reflecting the true efficacy of plasma treatment alone.

Table 1. Efficiency of non-thermal plasma on the inhibition of *C. neoformans* at various conditions

Input power	Mixed gas ratio	Efficiency of non-thermal plasma on The inhibition of *C. neoformans* - clear zone (cm^2)			
		30 s	1 min	2 min	3 min
30 W	Ar	0.04±0.002^{d4}	0.11±0.007^{c4}	0.24±0.018^{b3}	0.40±0.037^{a3}
	Ar:Air 1 LPM	0.26±0.017^{d3}	0.48±0.029^{c3}	0.71±0.046^{b2}	0.83±0.062^{a2}
	Ar:Air 1.5 LPM	0.33±0.021^{d2}	0.53±0.036^{c2}	0.77±0.069^{b1}	0.83±0.071^{a2}
	Ar:Air 2 LPM	0.40±0.027^{d1}	0.56±0.039^{c1}	0.76±0.038^{b1}	0.85±0.044^{a1}
50 W	Ar	0.07±0.006^{d4}	0.15±0.013^{c4}	0.27±0.019^{b3}	0.42±0.036^{a3}
	Ar:Air 1 LPM	0.42±0.025^{d3}	0.72±0.058^{c1}	0.83±0.056^{b1}	0.92±0.051^{a1}
	Ar:Air 1.5 LPM	0.47±0.033^{d2}	0.59±0.041^{c3}	0.81±0.053^{b2}	0.89±0.076^{a2}
	Ar:Air 2 LPM	0.53±0.040^{d1}	0.67±0.041^{c2}	0.82±0.057^{b1}	0.88±0.075^{a2}
70 W	Ar	0.08±0.005^{d4}	0.17±0.011^{c3}	0.28±0.020^{b3}	0.53±0.032^{a3}
	Ar:Air 1 LPM	0.48±0.036^{d3}	0.80±0.055^{c2}	0.86±0.056^{b1}	0.89±0.067^{a2}
	Ar:Air 1.5 LPM	0.51±0.041^{d2}	0.76±0.068^{c1}	0.82±0.065^{b2}	0.90±0.077^{a2}
	Ar:Air 2 LPM	0.59±0.050^{d1}	0.75±0.023^{c1}	0.83±0.079^{b2}	0.93±0.047^{a1}
Positive Control	Amphotericin B	2.20±0.045^{a}	2.45±0.056^{a}	3.10±0.062^{a}	3.25±0.081^{a}

Remark: Data are shown as mean ± SD of triplicated experiments; data with different lower-case superscript letters (a, b, c, and d) within the same row and data with different superscript numbers (1, 2, 3, and 4) within the same column of each condition are significantly different ($p < 0.05$).

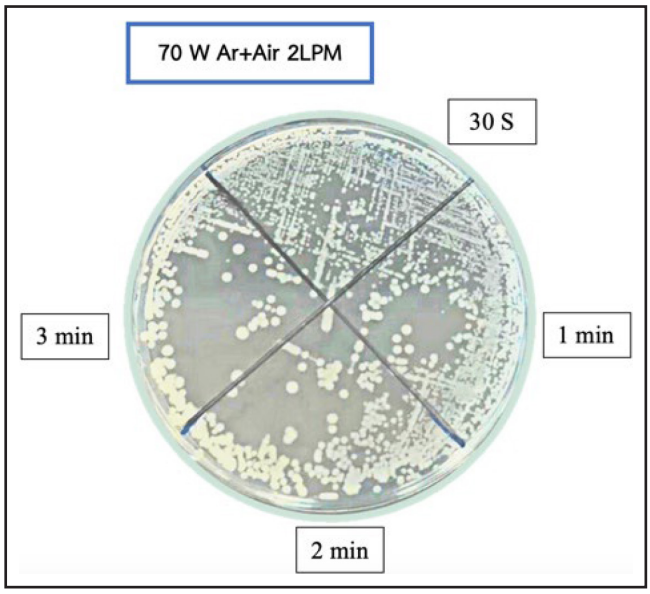

Figure 5. Inhibition of *C. neoformans* at 70 W Ar:Air 2 LPM.

The observed increase in colony size at longer exposure times might be attributed to the potential recovery or rapid regrowth capability of some surviving fungal cells after initial plasma exposure. This indicates a key limitation of relying solely on the clear zone measurement to accurately quantify antimicrobial efficacy, particularly when significant variations in treatment durations exist. Therefore, evaluating microbial inactivation through viable cell counts (Colony Forming Unit, CFU) would provide more precise and reliable results than clear zone measurements alone. CFU counts directly reflect the actual number of surviving fungal cells capable of growth post-treatment, thereby allowing a more accurate comparative analysis of the antimicrobial efficacy across different treatment conditions.

Jet temperature measurements, conducted using a contact thermocouple positioned beneath the jet nozzle at the agar surface, confirmed non-thermal plasma discharge under all experimental conditions. The recorded temperatures ranged from 28.0 ± 1.1 °C to 34.0 ± 1.6 °C, only slightly exceeding the ambient room temperature of 25.0 ± 1.2 °C maintained during experimentation. These temperatures are substantially below the thermal inactivation threshold for *Cryptococcus neoformans*, which requires exposure to 60 °C for at least 1 hour to achieve complete cell death and generate heat-killed, nonviable cells (Baronetti *et al*., 2006). No visual evidence of substrate melting, agar desiccation, or thermal degradation was observed. These findings confirm that the observed antifungal efficacy was predominantly mediated by plasma-generated reactive oxygen and nitrogen species (RONS), rather than by thermal effects.

Nevertheless, the clear zone method remains beneficial as an initial, rapid, and straightforward qualitative assessment of the antimicrobial effect of non-thermal plasma treatments. Given its practical advantages, it serves effectively in preliminary evaluations despite its limitations in quantitative accuracy. In this study, plasma exposures under different durations were applied to distinct sectors on the same agar plate to minimize biological variability. While the possibility of inter-sector diffusion of reactive species cannot be entirely ruled out, consistent differences in clear zone sizes across treatment durations suggest that direct plasma exposure was the dominant factor. For future studies, further validation and quantification using CFU methods are recommended to confirm and refine the current findings, ultimately enhancing the reliability and applicability of plasma-based antimicrobial strategies.

DISCUSSION

The comparative disinfection efficacy of different plasma gas compositions was evaluated through clearance zone analysis against *Cryptococcus neoformans*. Among the tested conditions, the combination of argon (Ar) with air exhibited markedly superior antimicrobial performance compared to pure argon. While pure Ar facilitates plasma formation at lower energy due to its inert nature, it inherently lacks chemically reactive species. The visible Ar plasma jet under such conditions appeared optically brighter but was less chemically active. In contrast, the addition of air to the Ar flow introduced molecular oxygen (O_2), nitrogen (N_2), and water vapor (H_2O), which significantly enriched the plasma chemistry. Reactive oxygen and nitrogen species (RONS), including O_3, OH, H_2O_2, HNO_3, HNO_2, and ONOOH, were primarily generated within the high-energy discharge zone between the electrodes. This configuration resulted in more effective ionization and a more chemically reactive plasma plume. These RONS are known to disrupt microbial structures and

biochemical processes, enhancing the inactivation efficiency (Nijdam *et al*., 2010; Ahn *et al*., 2014; Ishaq *et al*., 2014; Lu *et al*., 2014; Yan *et al*., 2017; Cheng, 2020; Nimbua *et al*., 2020; Su *et al*., 2021; Wei *et al*., 2023).

The enhanced efficacy of Ar-air plasma was particularly evident against *C. neoformans*, a pathogen characterized by a polysaccharide capsule composed of glucuronoxylomannan (GXM) and galactoxylomannan (GalXM). This capsule plays a crucial role in protecting the cell by restricting molecule penetration. However, RONS generated by the plasma jet–particularly OH, O_3, and H_2O_2—can compromise cell wall integrity, perforate the membrane, and lead to cytoplasmic leakage and eventual cell death (Zaragoza *et al*., 2009; Casadevall *et al*., 2019; Iyer *et al*., 2021). The optimal treatment parameters identified in this study were 70 W input power, 12:2 LPM Ar:Air ratio, and a 3-minute exposure time, which yielded a maximum inhibition zone of 0.93 ± 0.05 cm². Increased air concentration and prolonged exposure enhanced the generation of RONS, thereby improving antifungal performance. These findings are consistent with prior studies demonstrating the role of plasma-generated radicals in microbial inactivation (Sun *et al*., 2012; Guo *et al*., 2018).

Although the present study confirms the efficacy of non-thermal plasma against *C. neoformans*, one limitation is the absence of trials at input powers exceeding 70 W. Previous investigations have shown that higher power levels enhance RONS production and antimicrobial activity. However, elevating input power may introduce thermal effects and discharge instability, which must be carefully managed. Future studies should therefore include higher power levels and employ advanced diagnostics such as SEM, TEM, and molecular assays to investigate plasma-induced cellular damage and quantify reactive species generation.

The findings underscore the potential of non-thermal plasma as a chemical-free disinfection method, especially in urban environments where fungal contamination from pigeon droppings is prevalent. To translate laboratory results into practical applications, future research should focus on standardizing plasma parameters, performing quantitative microbial analyses, and assessing treatment performance under real-world conditions. Collaborations with public health and environmental agencies will be essential to evaluate feasibility, safety, and regulatory implications. A multidisciplinary approach integrating plasma physics, microbiology, and environmental science will be key to advancing non-thermal plasma technologies for public sanitation.

CONCLUSIONS

This study demonstrates the antifungal efficacy of non-thermal plasma (NTP) in inhibiting *C. neoformans* isolated from pigeon droppings under various experimental conditions. The most significant inactivation was observed at an input power of 70 W, using an argon-air gas flow ratio of 12:2 LPM and a 3-minute exposure time, resulting in a maximum inhibition zone of 0.93 ± 0.05 cm². These results underscore the potential of NTP as an environmentally friendly alternative to traditional antifungal agents. The generation of reactive oxygen and nitrogen species (RONS) by plasma jets is crucial for disrupting fungal cell structures, particularly the polysaccharide capsule of *C. neoformans*. However, limitations such as reliance on qualitative clear zone measurements and the lack of CFU quantification must be addressed in future research. Further investigations incorporating advanced imaging and biochemical analyses are recommended to enhance understanding of the inactivation mechanisms and optimize plasma parameters for practical applications in public and environmental health disinfection.

In light of the observed disinfection potential, non-thermal plasma should be further investigated for its applicability in public sanitation strategies especially in urban environments where fungal contamination from avian sources presents persistent health risks. Its chemical-free operation and ability to generate biologically active species in situ position NTP as a promising approach for enhancing microbial control protocols in environmentally sensitive and high-risk areas. Future efforts should explore operational integration in environmental settings through feasibility studies and stakeholder engagement.

ACKNOWLEDGEMENTS

The authors would like to express their sincere gratitude to the Department of Electrical Engineering, Faculty of Engineering, and the Department of Health Promotion, Faculty of Physical Therapy, Srinakharinwirot University, for their generous support in providing resources and laboratory facilities throughout the research period.

Conflict of Interest Statement

The author declares that they have no conflict of interests.

Funding

This research was financially supported by Srinakharinwirot University under the annual research grant program for the fiscal year 2022, in accordance with Contract No. 419/2565.

REFERENCES

Ahn, H.J., Kim, K.I., Hoan, N.N., Kim, C.H., Moon, E., Choi, K.S., Yang, S.S. & Lee, J.-S. (2014). Targeting cancer cells with reactive oxygen and nitrogen species generated by atmospheric-pressure air plasma. *PLIS ONE* **9**: e86173. https://doi.org/10.1371/journal.pone.0086173

Andriani, G.M., Spoladori, L.F.de.A., Fabris, M., Camargo, P.G., Pereira, P.M.L., Santos, J.P., Bartolomeu-Gonnalves, G., Alonso, L., Lancheros, C.A.C., Alonso, A. *et al*. (2023). Synergistic antifungal interaction of N-(butylcarbamothioyl) benzamide and amphotericin B against *Cryptococcus neoformans*. *Frontiers in Microbiology* **14**: 1040671. https://doi.org/10.3389/fmicb.2023.1040671

Baronetti, J. L., Chiapello, L. S., Aoki, M. P., Gea, S., & Masih, D. T. (2006). Heat killed cells of *Cryptococcus neoformans* var. *grubii* induces protective immunity in rats: immunological and histopathological parameters. *Medical Mycology* **44**: 493-504. https://doi.org/10.1080/13693780600750022

Buppan, P., Sommatas, A., Jinput, P., Pramongkol, N. & Sritawattpong, A. (2017). Isolation of University, *Cryptococcus neoformans* from avian droppings at Srinakharinwirot University Ongkharak Campus. *Srinakharinwirot Journal of Science and Technology* **9**: 128-135.

Casadevall, A., Coelho, C., Cordero, R.J.B., Dragotakes, Q., Jung, E., Vij, R. & Wear, M.P. (2019). The capsule of *Cryptococcus neoformans*. *Virulence* **10**: 822-831. https://doi.org/10.1080/21505594.2018.1431087

Chanchula, N., Pansuksan, K., Bootchanont, A., Wattanawikkam, C., Boonyawan, D. & Porjai, P. (2025). Investigating effect of cold plasma pretreatment on drying kinetics, bioactive compounds, and antibacterial properties of ginger slices. *Applied Food Research* **5**: 100900. https://doi.org/10.1016/j.afres.2025.100900

Chen, Z., Bai, F., Jonas, S.J. & Wirz, R.E. (2022). Cold atmospheric plasma for addressing the COVID 19 pandemic. *Plasma Processes and Polymers* **19**: 2200012. https://doi.org/10.1002/ppap.202200012

Cheng, H., Xu, J., Li, X., Liu, D. & Lu, X. (2020). On the dose of plasma medicine: equivalent total oxidation potential (ETOP). *Physics of Plasmas* **27**: 063514. https://doi.org/10.1063/5.0008881

Ding, W., Li, F. & Yang, L. (2009). Atmospheric-pressure glow discharge sustained by a resonant power supply. *IEEE Transactions on Plasma Science* **37**: 2207-2212. https://doi.org/10.1109/TPS.2009.2030202

Garcia-Cosio, G., Martinez, H., Calixto-Rodriguez, M. & Gomez, A. (2011). DC discharge experiment in an Ar/N2/CO2 ternary mixture: a laboratory simulation of the Martian ionosphere's plasma environment. *Journal of Quantitative Spectroscopy and Radiative Transfer* **112**: 2787-2793. https://doi.org/10.1016/j.jqsrt.2011.09.008

Guo, L., Xu, R., Gou, L., Liu, Z., Zhao, Y., Liu, D., Zhang, L., Chen, H. & Kong, M.G. (2018). Mechanism of virus inactivation by cold atmospheric-pressure plasma and plasma-activated water. *Applied and Environmental Microbiology* **84**: e00726-18. https://doi.org/10.1128/AEM.00726-18

Haertel, B., von Woedtke, T., Weltmann, K.-D. & Lindequist, U. (2014). Non-thermal atmospheric-pressure plasma possible application in wound healing. *Biomolecules & Therapeutics* **22**: 477-490. https://doi.org/10.4062/biomolther.2014.105

Handorf, O., Weihe, T., Bekeschus, S., Graf, A.C., Schnabel, U., Riedel, K. & Ehlbeck, J. (2018). Nonthermal plasma jet treatment negatively affects the viability and structure of *Candida albicans* SC5314 biofilms. *Applied and Environmental Microbiology* **84**: e01163-18. https://doi.org/10.1128/AEM.01163-18

He, T., Wang, Y., Chen, Z. & Zheng, Y. (2024). Discharge characteristics and reactive species diagnosis of a He + Ar + O2 plasma jet at atmospheric pressure. *European Physical Journal D* **78**: 80. https://doi.org/10.1140/epjd/s10053-024-00882-y

Ishaq, M., Evans, M. & Ostrikov, K. (2014). Effect of atmospheric gas plasmas on cancer cell signaling. *International Journal of Cancer* **134**: 1517-1528. https://doi.org/10.1002/ijc.28323

Ito, S., Sakai, K., Gamaleev, V., Ito, M., Hori, M., Kato, M. & Shimizu, M. (2020). Oxygen radical based on non-thermal atmospheric pressure plasma alleviates lignin-derived phenolic toxicity in yeast. *Biotechnology for Biofuels* **13**: 18. https://doi.org/10.1186/s13068-020-1655-9

Iyer, K.R., Revie, N.M., Fu, C., Robbins, N. & Cowen, L.E. (2021). Treatment strategies for cryptococcal infection: challenges, advances and future outlook. *Nature Reviews Microbiology* **19**: 454-466. https://doi.org/10.1038/s41579-021-00511-0

Joshi, S.G., Paff, M., Friedman, G., Fridman, G., Fridman, A. & Brooks, A.D. (2010). Control of methicillin-resistant *Staphylococcus aureus* in planktonic form and biofilms: a biocidal efficacy study of nonthermal dielectric-barrier discharge plasma. *American Journal of Infection Control* **38**: 293-301. https://doi.org/10.1016/j.ajic.2009.11.002

Krangvichain, P., Niyomtham, W. & Prapasarakul, N. (2016). Occurrence and susceptibilities to disinfectants of *Cryptococcus neoformans* in fecal droppings from pigeons in Bangkok, Thailand. *Journal of Veterinary Medical Science* **78**: 391-396. https://doi.org/10.1292/jvms.15-0594

Lu, X., Naidis, G.V., Laroussi, M. & Ostrikov, K. (2014). Guided ionization waves: theory and experiments. *Physics Reports* **540**: 123-166. https://doi.org/10.1016/j.physrep.2014.02.006

Madsen, A.M., White, J.K., Nielsen, J.L., Keskin, M.E., Tendal, K. & Frederiksen, M.W. (2022). A cross sectional study on airborne inhalable microorganisms, endotoxin, and particles in pigeon coops – risk assessment of exposure. *Environmental Research* **204**: 112404. https://doi.org/10.1016/j.envres.2021.112404

Matra, K., Aryuwong, W., Meetang, W., Ruthairat, S., Dechthummarong, C., Sangwang, W. & Luang-In, V. (2023). Application of electrical breakdown in liquid process on inulin structural transformations. *IEEE Access* **11**: 114777-114789. https://doi.org/10.1109/ACCESS.2023.3321339

Matra, K., Zonklin, B., Hamkratok, S. & Pachekrepapol, U. (2025). Effect of dielectric barrier discharge cold plasma combined with green tea extract on quality and safety of ready-to-eat fish patties during storage. *Discover Food* **5**: 46. https://doi.org/10.1007/s44187-025-00320-x

Morabit, Y., Hasan, M.I., Whalley, R.D., Robert, E., Modic, M. & Walsh, J.L. (2021). A review of the gas and liquid phase interactions in low-temperature plasma jets used for biomedical applications. *European Physical Journal D* **75**: 32. https://doi.org/10.1140/epjd/s10053-020-00004-4

Morrison, V.A. (2006). Echinocandin antifungals: review and update. *Expert Review of Anti-Infective Therapy* **4**: 325-342. https://doi.org/10.1586/14787210.4.2.325

Morrow, C.A. & Fraser, J.A. (2013). Is the Nickel-dependent uease complex of *Cryptococcus* the pathogen's achilles' heel? *mBio* **4**: 10.1128/mBio.00408-13. https://doi.org/10.1128/mBio.00408-13

Nijdam, S., van De Wetering, F.M.J.H., Blanc, R., van Veldhuizen, E.M. & Ebert, U. (2010). Probing photo-ionization: experiments on positive streamers in pure gases and mixtures. *Journal of Physics D: Applied Physics* **43**: 145204. https://doi.org/10.1088/0022-3727/43/14/145204

Nimbua, S., Pluksa, C., Temponsub, T., Thabin, P., Buppan, P. & Matra, K. (2020). The influence of Argon, Oxygen, and Air plasma jet on *Escherichia coli* inactivation. Proceedings of the 8th International Electrical Engineering Congress 2020 (IEECON), pp. 1-4. https://doi.org/10.1109/iEECON48109.2020.229566

Niu, Z., Shao, T., Zhang, C., Jiang, H., Li, C., Wang, G., Tan, J. & Yan, P. (2011). Atmospheric-pressure plasma jet produced by a unipolar nanosecond pulse generator in various gases. *IEEE Transactions on Plasma Science* **39**: 2322-2323. https://doi.org/10.1109/TPS.2011.2127495

Pal, N., Sinha, R., Ray, R., Chakraborty, A., Banu, H. & Dutta, S. (2024). A rare case of histoplasma and cryptococcus coinfection in an apparently immunocompetent child. *Journal of Dr. YSR University of Health Sciences* **13**: 403-406. https://doi.org/10.4103/jdrysruhs.jdrysruhs_71_22

Palee, N., Thana, P., Wijaikham, A., Pussadee, N. & Boonyawan, D. (2023). Modeling simulation of nitric oxide and ozone generated by the Compact Air Plasma Jet: Nightingale®. *Journal of Physics: Conference Series* **2653**: 012067. https://doi.org/10.1088/1742-6596/2653/1/012067

Pan, H., Wang, G., Jie, P., Ye, G., Sun, K., Zhang, J. & Wang, J. (2015). Cold plasma-induced surface modification of heat-polymerized acrylic resin and prevention of early adherence of *Candida albicans*. *Dental Materials Journal* **34**: 529-536. https://doi.org/10.4012/dmj.2015-035

Panklai, T., Kumchaiseemak, N., Seelarat, W., Sangwanna, S., Chutimayanaphat, C., Bootchanont, A., Wattanawikkam, C., Rittidach, T., Boonyawan, D. & Porjai, P. (2025). Investigating effects of air-cold plasma jet on enzymatic activity and nutritional quality attributes of Mangosteen (*Garcinia mangostana* L.) juice. *Innovative Food Science and Emerging Technologies* **99**: 103878. https://doi.org/10.1016/j.ifset.2024.103878

Qayyum, A., Zeb, S., Naveed, M.A., Rehman, N.U., Ghauri, S.A. & Zakaullah, M. (2007). Optical emission spectroscopy of Ar–N2 mixture plasma. *Journal of Quantitative Spectroscopy and Radiative Transfer* **107**: 361-371. https://doi.org/10.1016/j.jqsrt.2007.02.008

Seelarat, W., Sangwanna, S., Chaiwon, T., Panklai, T., Chaosuan, N., Bootchanont, A., Wattanawikkam, C., Porjai, P., Khuangsatung, W. & Boonyawan, D. (2024). Impact of pretreatment with dielectric barrier discharge plasma on the drying characteristics and bioactive compounds of jackfruit slices. *Journal of the Science of Food and Agriculture* **104**: 3654-3664. https://doi.org/10.1002/jsfa.13250

Shi, J., Jin, B., Ma, S., Liu, X., Leng, X. & Chen, K. (2023). Microanalysis of Active Nitrogen Oxides (RONS) generation characteristics during DC negative corona discharge at a needle-plate electrode. *Plasma* **6**: 649-662. https://doi.org/10.3390/plasma6040045

Su, C.-F., Liu, C.-T., Wu, J.-S. & Ho, M.-T. (2021). Development of a High-Power-Factor power supply for an atmospheric-pressure plasma jet. *Electronics* **10**: 2119. https://doi.org/10.3390/electronics10172119

Sun, Y., Yu, S., Sun, P., Wu, H., Zhu, W., Liu, W., Zhang, J., Fang, J. & Li, R. (2012). Inactivation of *Candida* biofilms by non-thermal plasma and its enhancement for fungistatic effect of antifungal drugs. *PLOS ONE* **7**: e40629. https://doi.org/10.1371/journal.pone.0040629

Thana, P., Boonyawan, D., Jaikua, M., Promsart, W., Rueangwong, A., Ungwiwatkul, S., Prasertboonyai, K. & Maitip, J. (2025a). Plasma-Activated Water (PAW) decontamination of foodborne bacteria in shucked oyster meats using a compact flow-through generator. *Foods* **14**: 1502. https://doi.org/10.3390/foods14091502

Thana, P., Jaikua, M., Maitip, J., Ungwiwatkul, S., Prasertboonyai, K., Rueangwong, A. & Promsart, W. (2025b). Exploring potential of a Remote Plasma Electrolysis System (RPES) for fruit surface sterilization. *E3S Web of Conferences* **602**: 02009. https://doi.org/10.1051/e3sconf/202560202009

Ungwiwatkul, S., Jaikua, M., Prasertboonyai, K., Thana, P., Tamman, A. & Matra, K. (2025). Plasma-Activated Municipal Wastewater (PAMW): revolutionizing municipal wastewater into high-value liquid fertilizer for duckweed cultivation through air plasma treatment. *Applied Science and Engineering Progress* **18**: 7791. https://doi.org/10.14416/j.asep.2025.04.002

Wang, H.S., Zeimis, R.T. & Roberts, G.D. (1977). Evaluation of a caffeic acid-ferric citrate test for rapid identification of *Cryptococcus neoformans*. *Journal of Clinical Microbiology* **6**: 445-449. https://doi.org/10.1128/jcm.6.5.445-449.1977

Watkins, R.A., King, J.S. & Johnston, S.A. (2017). Nutritional requirements and their importance for virulence of pathogenic *Cryptococcus* species. *Microorganisms* **5**: 65. https://doi.org/10.3390/microorganisms5040065

Wei, Z., Komuro, A. & Ono, R. (2023). Simulation study on influence of oxygen concentrations on atmospheric-pressure streamer in oxygen-rich nitrogen-oxygen mixture. *Plasma Sources Science and Technology* **32**: 115016. https://doi.org/10.1088/1361-6595/ad0b97

Xu, G.-M., Ma, C.-Q., Song, Y.-H., Wang, X.-Y., Liu, J.-R., Wang, X.-N., Cui, Y.-X., Lu, J.-J., Kang, C.-C., Li, L.-J. *et al*. (2024). Inactivation mechanisms of pulsed corona discharge plasma on *Escherichia coli* and *Staphylococcus aureus* Phages. *IEEE Transactions on Plasma Science* **52**: 1947-1955. https://doi.org/10.1109/TPS.2023.3297572

Yan, D., Cui, H., Zhu, W., Nourmohammadi, N., Milberg, J., Zhang, L.G., Sherman, J.H. & Keidar, M. (2017). The specific vulnerabilities of cancer cells to the cold atmospheric plasma-stimulated solutions. *Scientific Reports* **7**: 4479. https://doi.org/10.1038/s41598-017-04770-x

Zaragoza, O., Rodrigues, M.L., De Jesus, M., Frases, S., Dadachova, E. & Casadevall, A. (2009). Chapter 4 The capsule of the fungal pathogen *Cryptococcus neoformans*. *Advances in Applied Microbiology* **68**: 133-216. https://doi.org/10.1016/S0065-2164(09)01204-0

Zhao, Y., Ye, L., Zhao, F., Zhang, L., Lu, Z., Chu, T., Wang, S., Liu, Z., Sun, Y., Chen, M. *et al*. (2023). *Cryptococcus neoformans*, a global threat to human health. *Infectious Diseases of Poverty* **12**: 1-18. https://doi.org/10.1186/s40249-023-01073-4